A self-consistent three-wave coupling model with complex linear frequencies

J.-H. Kim[a)] and P. W. Terry
Department of Physics, University of Wisconsin-Madison, Madison, Wisconsin 53706, USA

A three-wave coupling model with complex linear frequencies is investigated for the nonlinear interaction in a triad that has linearly unstable and stable modes. Time scales associated with linear and nonlinear physics are identified and compared with features of the frequency spectrum. From appropriate time scales, the frequency spectra are well characterized even in the transition to the steady state. The nonlinear time scales that best match spectral features are the nonlinear frequency of the fixed point and a frequency that depends on the amplitude displacement from the fixed point through the large-amplitude Jacobian elliptic solution. Two limited efforts to model the effect of other triads suggest robustness in the single triad results. © *2011 American Institute of Physics*. [doi:10.1063/1.3640807]

I. INTRODUCTION

The wave triad interaction is the smallest irreducible element of the nonlinear dynamics of plasmas and fluids with quadratic nonlinearity.[1–3] Even though the isolated triad interaction has limitations in its ability to represent turbulence, where many triads couple to each other, the dynamical properties of this coupling have been studied in the context of intrinsic three wave processes (i.e., parametric instability[4]), as a test bed of a turbulent closure theory,[5,6] and for probing energy cascades (or more generally, inferring the direction of nonlinear energy transfer among modes in turbulence).[7,8] Most importantly and comprehensively, this interaction has been investigated as a conceptual building block for understanding turbulence, both weak[3,9] and strong.[5,6,10,11] Three-wave coupling models show a variety of dynamics depending on the specification of parameters. Often, stochasticity[5,12] and integrability[13] have been the focus of attention. Weiland and Wilhelmsson[1] can be referred to for a comprehensive description of the coherent aspects of nonlinear wave-wave interactions.

One area where the study of the isolated triad interaction potentially has much to offer is in understanding the turbulent frequency spectrum at fixed wavenumber. This quantity, which in principle, is easy to measure in plasmas because of the relative ease of collecting ensembles in the time domain, has been underutilized. Such measurements are not as common as they could be, despite the potential for providing detailed information on turbulent dynamics, and stringent tests of model fidelity for validation. One reason for the underutilization of this measurement is the lack of theoretical understanding. The wavenumber spectrum has mappings from scales of known processes and, in cases where it is most used, power law behavior that relates directly to nonlinearity through familiar theoretical constructs. The fixed wavenumber frequency spectrum is constructed to have similar points of contact with physical processes. However, it has never been settled what frequencies ought to apply, or what

imprint is imposed by the nonlinearity. Features, like spectral widths that significantly exceed the nonlinear decorrelation rate, do not square with theory, and are common. Attempts to develop theoretical underpinnings have been sparse, limited, and not very satisfactory (for a discussion see Sec. I of Mattor and Terry[14]).

Recent studies of plasma turbulence that account for the spectrum of "damped" modes offer important new insights about the mode frequency input to plasma turbulence. These studies have shown that damped modes play a key role in saturated turbulence even at the length scales of instability, far from dissipation ranges.[15–20] Damped modes can produce significant effects not before anticipated, like ergodization of the magnetic field.[18] At each wavenumber, damped modes are excited by the nonlinearity in large numbers,[18] and most carry a real frequency (see Fig. 2 of Hatch *et al.*[20]). Consequently, there are far more linear frequencies potentially entering the frequency spectrum at fixed wavenumber than previously believed. An effort to match the anomalously broad fixed-wavenumber frequency spectrum of ion temperature gradient mode (ITG) turbulence in GYRO (Ref. 21) with the limited number of damped mode frequencies provided by a reduced gyro Landau fluid model[22] has showed some promise.[16] If damped mode frequencies could be definitively matched to frequency spectrum features, it would provide a diagnostic for the damped mode spectrum. However, comparisons of the frequency spectrum with the much larger number of damped mode frequencies provided by a gyrokinetic eigenmode solver[23] have indicated that the link is much more complicated. It appears that more work is needed in understanding the effect of the nonlinearity in the frequency spectrum arising from a spectrum of damped modes.

When fluctuations are decomposed into unstable and damped mode components, it is found that energy injected by linearly unstable modes is nonlinearly transferred to stable modes at comparable wavenumbers. The direction of energy transfer seems to be extremely consistent in the energetically dominant wavenumbers, such that time averages are not required to see a consistent directionality. The consistency hints that a coherent nonlinear dynamics can be

a)Electronic mail: jkim282@wisc.edu.

     18, 092308-1

uncovered. The coherent dynamics are part of the effect of the nonlinearity in the frequency spectrum, and represent a primary focus of this paper.

To make the complexities intrinsic to the frequency spectrum more manageable, it is sensible to examine the frequency spectrum of an isolated triad as it relates to the linear frequencies of each mode and the triad interaction's more transparent nonlinear time scales. Hence this paper undertakes an inventory of frequencies, linear and nonlinear, that can be identified in triad interactions, and examines their relationship with the frequency spectrum of stationary three-wave evolution. We investigate the three-wave frequency spectrum among linearly unstable and stable modes using a simple model where only coherent nonlinear dynamics is present and stochasticity is absent. This system is "self-consistent" in the sense that the amplitudes of the modes in a triad are determined by the nonlinear interactions among the modes. Consequently, the nonlinear time scale, given approximately by $N(\phi)/(d\phi/dt)$, where N is a nonlinear term in the evolution of the amplitudes ϕ, is not prescribed. The system evolves into an energetically steady state by adjusting its phase evolution and amplitudes. Each mode has a nonlinear frequency $\hat{\omega}$ that is nonlinearly shifted from the linear frequency ω. The nonlinear frequencies of a triad satisfy the frequency matching condition $\Delta\hat{\omega} = 0$, even though the linear frequencies $\Delta\omega \neq 0$ do not. (The notation will be clearly defined later.) Only certain three-wave couplings can have a stable equilibrium state (which we henceforth call a stable fixed point of a triad). Near the fixed point, the frequency modification of each mode can be heuristically estimated by the distance of the mode amplitude from the fixed point. It is shown that a stable fixed point can be robust to certain perturbations. This work answers what a dynamically coherent feature is when the nonlinear energy transfer is subjected to the balance between linearly unstable and stable modes.

The paper is organized as follows: the model is presented in Sec. II; the fixed point and its linear stability are examined in Sec. III; the saturation and the relaxation are given numerically in Sec. IV; the frequency comparison is presented in Sec. V; and the triad perturbed by an external fluctuation and two triad interactions are treated in Sec. VI. The conclusion and discussion are given in Sec. VII.

II. MODEL EQUATION

Isolated triad interactions with quadratic nonlinear coupling satisfy the general equation

$$\frac{d\phi_i}{dt}(t) + i\lambda_i\phi_i(t) = M_i\phi_j^*(t)\phi_k^*(t), \quad i = 1, 2, 3, \quad (1)$$

where (i, j, k) are the permutations of $(1, 2, 3)$ and ϕ is complex. A complex linear coefficient $\lambda_i = \omega_i + i\gamma_i$ represents the linear frequency ω_i and the linear growth rate γ_i of a mode i. Each mode i interacts nonlinearly with modes j and k, with the interaction strength governed by the complex nonlinear coefficient $M_i = M_{ijk}$. No summation over the indexes i, j, k is assumed. For concreteness, we label modes so that $\gamma_1 > \gamma_2 > \gamma_3$. This model equation has been used to study the

triad interaction of drift wave turbulence[5] and turbulence closure theory.[6]

The quadratic function $|\phi_i|^2$ is called the energy, and its temporal evolution is governed by

$$\frac{1}{2}\frac{d}{dt}|\phi_i|^2 = \gamma_i|\phi_i|^2 + \text{Re}\left\{M_i\phi_i^*\phi_j^*\phi_k^*\right\}. \quad (2)$$

The energy evolution of a mode is governed by the linear energy growth or damping and the nonlinear energy transfer.

A necessary and sufficient condition for preserving energy conservation by the nonlinearity is that the nonlinear interaction strength M_i satisfy

$$\text{Re}\{M_1 + M_2 + M_3\} = 0 \text{ and } \text{Im}\{M_1 + M_2 + M_3\} = 0. \quad (3)$$

Here we will assume that M_i is real. The complex nonlinear coefficients M_i due to the ion polarization drift in the Terry-Horton model for trapped electron mode turbulence lead to a stochastic system.[5] Purely real or purely imaginary nonlinear interaction coefficients M_i describe advection of vorticity in the Navier-Stokes equation or the $\boldsymbol{E} \times \boldsymbol{B}$ advection in the Hasegawa-Mima model of electron drift waves in strongly turbulent plasmas.[24]

Let us compare the coupling model to the Hasegawa-Mima equation and a two-field plasma turbulence model in order to make its limits clear. The Hasegawa-Mima equation is a one-field model of electron drift wave turbulence. It has negative growth rate $\gamma_i < 0$ and real M_i for all i. Allowing for instability requires the additional inclusion of an ad hoc positive linear growth rate. A two-field model can have instability. However each wave vector $\boldsymbol{k}$ has two linear eigenvectors, either stable-stable or stable-unstable. Two waves of the same $\boldsymbol{k}$ are not orthogonal so that the minimum unit of self-sufficient nonlinear interaction is among six modes, two modes per each $\boldsymbol{k}$. The resulting equation for mode evolution then has two nonlinear terms with nonlinear coefficients that depend on the linear eigenvectors. Our model with real M_i can be thought of as a modified Hasegawa-Mima equation that avoids intrinsic stochasticity and higher order wave interactions.

Separation of time scales in wave turbulence studies generally requires weak growth relative to linear frequency, $\gamma_{\text{lin}} \ll \omega_0$ and a stochastic phase distribution (random phases), represented by $\phi = \Phi(t)e^{i\theta(\tau)}$, where $\tau = t/\epsilon$ and ϵ is small. Resonant mode interactions with $\Delta\omega = 0$ thus play a role in the dynamics. Wave action is conserved on the slow time scale. However, to achieve the saturation, nonlinear diffusion should be included. Saturation is then achieved by a balance between the unstable mode growth rate γ_i and the nonlinear diffusion. In comparison, no separation of time scales is assumed in this study and $\omega_i \sim \gamma_i$ is allowed.

The total energy ΔE of the triad evolves as

$$\frac{d\Delta E}{dt} = \frac{d}{dt}\left[\frac{1}{2}\sum_{i=1}^{3}|\phi_i|^2\right] = \sum_{i=1}^{3}\gamma_i|\phi_i|^2. \quad (4)$$

In the steady state, this reduces to the algebraic relation

$$\gamma_1|\phi_1|^2 + \gamma_2|\phi_2|^2 + \gamma_3|\phi_3|^2 = 0. \quad (5)$$

To reach a steady state within a triad, the triad must consist of two unstable modes and one stable mode (*uus*) or one unstable mode and two stable modes (*uss*). A triad (*uus*) or (*uss*) is the smallest unit of nonlinear interaction that can satisfy the steady state energy relation, Eq. (5).

We introduce the representation

$$\phi_i(t) = \Psi_i(t)e^{-i\psi_i(t)}, \tag{6}$$

where two real quantities Ψ_i and ψ_i represent the amplitude and the phase of the complex mode amplitude ϕ_i. Equation (1) can be rewritten as

$$\frac{d\Psi_i}{dt} = \gamma_i\Psi_i + \Psi_j\Psi_k M_i \cos\Delta\psi \tag{7}$$

$$\frac{d\psi_i}{dt} = \omega_i - \frac{\Psi_j\Psi_k}{\Psi_i}M_i \sin\Delta\psi. \tag{8}$$

Notice that the nonlinear evolution of the mode amplitude Ψ_i and the mode phase ψ_i are governed not by the individual phase of a mode, but by the triad phase, $\Delta\psi(t) = \sum_i \psi_i(t)$. The evolution of the triad phase is given by

$$\frac{d\Delta\psi}{dt} = \Delta\omega - \sum_{P(i,j,k)} \frac{\Psi_j\Psi_k}{\Psi_i}M_i \sin\Delta\psi, \text{ or} \tag{9a}$$

$$\frac{d\Delta\psi}{dt} = \Delta\omega + \tan\Delta\psi\left[\Delta\gamma - \frac{d}{dt}\log(\Psi_1\Psi_2\Psi_3)\right], \tag{9b}$$

where the total linear frequency $\Delta\omega$ and the total growth rate $\Delta\gamma$ are

$$\Delta\omega = \sum_i \omega_i \quad \text{and} \quad \Delta\gamma = \sum_i \gamma_i.$$

The Eqs. (7) and (9) are sufficient to represent the evolution of the triad, Ψ_i and $\Delta\psi$.

III. TRIAD FIXED POINT AND STABILITY

To find a fixed point, Eq. (7) is set to zero, which requires that Eq. (9) be zero. The mode amplitudes Ψ_{0i} at the fixed point are given by

$$\Psi_{0i}^2 = \frac{\gamma_j\gamma_k}{M_jM_k\cos^2\Delta\psi} = \left|\frac{M_i}{\gamma_i}\right|\frac{|\Gamma_3|}{H^2}\left(1 + \frac{\Delta\omega^2}{\Delta\gamma^2}\right)$$
$$= p\frac{M_i}{\gamma_i}\frac{|\Gamma_3|}{H^2}\left(1 + \frac{\Delta\omega^2}{\Delta\gamma^2}\right), \tag{10}$$

where $\Gamma_3 = \gamma_i\gamma_j\gamma_k$, $H = \sqrt{|M_iM_jM_k|}$, the triad phase is

$$\tan\Delta\psi_0 = -\frac{\Delta\omega}{\Delta\gamma} \text{ or } \cos\Delta\psi_0 = p\frac{|\Delta\gamma|}{\sqrt{\Delta\omega^2 + \Delta\gamma^2}}, \tag{11}$$

and $p = sgn(\tan\Delta\psi_0) = sgn(-\Delta\omega/\Delta\gamma)$. It can be verified that steady state requires $M_i/\gamma_i = p|M_i/\gamma_i|$, or equivalently,

$$p = sgn(\gamma_1 M_1) = sgn(\gamma_2 M_2) = sgn(\gamma_3 M_3) = \pm 1. \tag{12}$$

These expressions guarantee that $\gamma_j\gamma_k/M_jM_k \sim \Psi_{0i}^2 > 0$, consistent with real amplitudes Ψ_{0i}.

Since $M_1 + M_2 + M_3 = 0$, one M_i has an opposite sign to the other two. The equality $p = sgn(\gamma_i M_i)$ for all i is consistent with Eq. (5), i.e., steady state requires that the triad should be (*uss*) or (*uus*), except for the trivial solution (0, 0, 0). The equality $p = sgn(\gamma_i M_i)$ also provides a possible combination of $\mathbf{k}_i$ in addition to $\mathbf{k}_i + \mathbf{k}_j + \mathbf{k}_k = 0$ when $M_i = M_i(\mathbf{k}_j, \mathbf{k}_k)$. For example, in the Hasegawa-Mima model,[24] the nonlinear coefficient is given by

$$M_i \sim -\mathbf{k}_j \times \mathbf{k}_k\left(\mathbf{k}_j^2 - \mathbf{k}_k^2\right).$$

For the triad (*uss*) where $\gamma_1 > 0 > \gamma_2 > \gamma_3$, the condition $sgn(\gamma_i M_i) = p$ for all i leads to

$$|\mathbf{k}_2| < |\mathbf{k}_1| < |\mathbf{k}_3| \text{ or } |\mathbf{k}_3| < |\mathbf{k}_1| < |\mathbf{k}_2|.$$

These relation permit coherent nonlinear transfer from an unstable mode of intermediate wavenumber to the stable modes of smaller and larger wavenumbers. This wavenumber relation prevents coherent nonlinear energy transfer from an unstable mode of small wavenumber to two stable modes of large wavenumber, i.e., $k_1 < k_2 < k_3$. For the triad (*uus*), where $\gamma_1 > \gamma_2 > 0 > \gamma_3$, the wavenumber vectors in a triad should satisfy

$$|\mathbf{k}_1| < |\mathbf{k}_3| < |\mathbf{k}_2| \text{ or } |\mathbf{k}_2| > |\mathbf{k}_3| > |\mathbf{k}_1|.$$

Coherent nonlinear energy transfer from two unstable modes to a stable mode is possible only when the wavenumber of the stable mode is intermediate to the wavenumbers of the unstable modes.

From Eq. (10), the relative amplitudes of three modes in the steady state are

$$\Psi_{01} : \Psi_{02} : \Psi_{03} = \sqrt{\left|\frac{M_1}{\gamma_1}\right|} : \sqrt{\left|\frac{M_2}{\gamma_2}\right|} : \sqrt{\left|\frac{M_3}{\gamma_3}\right|}, \tag{13}$$

and the energy damping (injection) rate of each mode is proportional to the nonlinear coefficients M_i,

$$\gamma_1\Psi_1^2 : \gamma_2\Psi_2^2 : \gamma_3\Psi_3^2 = M_1 : M_2 : M_3. \tag{14}$$

Assuming $M_1 \sim M_2 \sim M_3$ and $0 > \gamma_2 \gg \gamma_3, -\gamma_1$, the amplitude of the mode 2 is relatively large but its energy damping rate is of the same order as the rates of the other modes. We note that the solution of this model is obtained in Bowman *et al.*[6]

The fixed-point amplitudes are dependent on the triad phase. The triad phase depends only on the ratio of the total linear frequency $\Delta\omega$ to the total linear growth rate $\Delta\gamma$. A non-resonant triad, $\Delta\omega \neq 0$, has a larger value of $\tan\Delta\psi_0$ and a smaller value of $\cos\Delta\psi_0$ than a resonant triad, $\Delta\omega = 0$, assuming the rest of the parameters are equal. For the non-resonant triad, weak nonlinear interaction due to small $\cos\Delta\psi_0$ requires large amplitudes Ψ_{0i}. At the fixed point, the amplitudes of a non-resonant triad are larger by a factor of $\sqrt{(1 + \Delta\omega^2/\Delta\gamma^2)}$ than the amplitudes of a resonant triad.

Because a mode phase is dependent on the mode amplitude and the triad phase, the phase velocity of a mode at the

fixed point can be obtained by substituting Eqs. (10) and (11) into Eq. (8). The phase velocity, or nonlinear frequency, of each mode at the fixed point is the linear frequency ω_i shifted nonlinearly by $\gamma_i \tan \Delta\psi_0$,

$$\hat{\omega}_i \equiv \frac{d\psi_i}{dt} = \omega_i + \gamma_i \tan \Delta\psi_0 = \omega_i - \gamma_i \frac{\Delta\omega}{\Delta\gamma}. \quad (15)$$

In turbulence, finite amplitudes shift mode frequencies from the linear frequency through amplitude oscillation or wave-phase modification. Nonlinear frequency shifts are generally obtained in a perturbative way.[25–27] Here, the energy constraint and the low-order ordinary differential equations (ODEs) of the isolated three-wave model enable a non-perturbative calculation of the nonlinear frequency shift. The nonlinear frequency $\hat{\omega}_i$ of the fixed point is relevant to the eigen-frequency of a nonlinear dispersion relation (for example, Hinton and Horton[25]). Since the triad phase at a fixed point is constant in time, a non-resonant triad adjusts individual phase velocities to satisfy nonlinear resonance $\Delta\hat{\omega} = 0$, as well as the energy balance of Eq. (5). In the limiting case of $\Delta\omega \gg \Delta\gamma$, the nonlinear frequency shift $-\gamma_i(\Delta\omega/\Delta\gamma) \gg \omega_i$ governs the frequency of a mode at a fixed point. The frequency of the mode in a resonant triad is the linear frequency of the mode ω_i with no nonlinear shift. In addition, it is worth noting that even a zero-frequency mode can have finite frequency through coherent nonlinear interaction.

The next step is to investigate the stability of the fixed point. The steady state is a fixed point in the four dimensional phase space of $(\boldsymbol{\Psi}, \Delta\psi)$, but it is a limit cycle in the six-dimensional phase space of $(\boldsymbol{\Psi}, \psi)$. Here the linear stability of the fixed point is explored. The linearized equations are given by

$$\frac{d}{dt}\frac{\delta\Psi_i}{\Psi_{0i}} = \gamma_i\left(\frac{\delta\Psi_i}{\Psi_{0i}} - \frac{\delta\Psi_j}{\Psi_{0j}} - \frac{\delta\Psi_k}{\Psi_{0k}} + \delta\Delta\psi \tan\psi_0\right), \quad (16a)$$

$$\frac{d}{dt}\delta\Delta\psi = \Delta\gamma\delta\Delta\psi + \sum_i (\Delta\gamma - 2\gamma_i)\frac{\delta\Psi_i}{\Psi_{0i}}\tan\psi_0. \quad (16b)$$

The fourth order characteristic polynomial equation for the frequency σ of the normal mode solution $\delta\Psi_i/\Psi_{0i} = A_i \exp(\sigma t)$ is

$$\sigma^4 - 2\Delta\gamma\sigma^3 + \left[\sec^2\psi_0\Delta\gamma^2 - 4\tan^2\psi_0\Gamma_2\right]\sigma^2$$
$$+ 4\Gamma_3(1 + 3\tan^2\psi_0)\sigma - 4\Gamma_3\Delta\gamma(1 + \tan^2\psi_0) = 0, \quad (17)$$

where $\Gamma_2 = \gamma_1\gamma_2 + \gamma_2\gamma_3 + \gamma_3\gamma_1$. When $\Delta\gamma > 0$, the fixed point is always unstable. The stability depends not on the individual linear frequencies ω_i but only on the linear growth rates γ_i and the ratio $\Delta\omega/\Delta\gamma$, which determines the strength of the nonlinear interaction, and the nonlinear frequency shift. From now on, we assume that $\Delta\gamma < 0$.

A. Resonant triad $\Delta\omega = 0$

Because $\tan\psi_0 = 0$ and $\sec^2\psi_0 = 1$, the characteristic polynomial becomes

$$(\sigma - \Delta\gamma)(\sigma^3 - \Delta\gamma\sigma^2 + 4\Gamma_3) = 0. \quad (18)$$

There are three characteristic frequencies in addition to $\sigma = \Delta\gamma < 0$. These consist of a real root $\sigma_1 < 0$, and a complex conjugate pair σ_2 and σ_2^*. For the triad (uss), $\Gamma_3 > 0$, yielding

$$\sigma_1 < 0 \text{ and } \text{Re}\,\sigma_2 > 0,$$

since $\gamma_1|\gamma_2|^2 < 0$ and $2\sigma_1\text{Re}\sigma_2 + |\sigma_2|^2 = 0$. For the triad (uus), $\Gamma_3 < 0$, yielding

$$\sigma_1 > 0 \text{ and } \text{Re}\,\sigma_2 < 0.$$

We conclude that there is always at least one characteristic frequency with a positive real part. Hence the fixed point of a resonant triad is always unstable.

B. Non-resonant triad $\Delta\omega \neq 0$

The stability of non-resonant triads is more difficult to solve. In the limit of $|\Delta\gamma| \gg |\Delta\omega|$, the non-resonant triad is unstable like the resonant triad. In the opposite limit of $|\Delta\gamma| \ll |\Delta\omega|$, we assume that

$$\Delta\gamma, \Gamma_2 \sim O(\epsilon); \quad \Gamma_3 \sim O(\epsilon^2); \quad \text{and} \quad \Delta\omega \sim O(1), \quad (19)$$

where ϵ is a small parameter. The set of the parameters in Sec. IV satisfy this ordering assumption. In this case, there are fast and slow pairs of characteristic frequency solutions. Fast and slow refer to the imaginary part $\text{Im}\,\sigma$ of the characteristic frequencies for motion near a fixed point. The fast frequency is $\sigma_f = \sum_{n=-1,\infty} \hat{\sigma}_{f,n/2}\epsilon^{n/2}$, where

$$\hat{\sigma}_{f,-1/2} = \pm\sqrt{4\Gamma_2\frac{\Delta\omega^2}{\Delta\gamma^2}},$$

$$\hat{\sigma}_{f,0} = 0,$$

$$\hat{\sigma}_{f,1/2} = -\frac{\Delta\omega^2}{2\hat{\sigma}_{f,-1/2}},$$

and

$$\hat{\sigma}_{f,1} = \Delta\gamma - \frac{3\Gamma_3}{2\Gamma_2}.$$

The fixed point is unstable with a large real positive eigen-frequency $\text{Re}\,\sigma \sim O(1/\sqrt{\epsilon})$ for $\Gamma_2 > 0$, and stable with a fast eigen-frequency $\text{Im}\,\sigma \sim O(1/\sqrt{\epsilon})$ for $\Gamma_2 < 0$. For $\Gamma_2 < 0$, the stability condition is determined up to $O(\epsilon) \sim \Delta\gamma$ as $\Delta\gamma_2 < 3\Gamma_3/\Gamma_2$.

The slow characteristic eigen-frequencies for motion near a fixed point are $\sigma_s = \sum_{n=1,\infty} \hat{\sigma}_{s,n}\epsilon^n$, where

$$\hat{\sigma}_{s,1} = \frac{3\Gamma_3 \pm \sqrt{\Gamma_3(9\Gamma_3 - 4\Delta\gamma\Gamma_2)}}{2\Gamma_2}, \quad \text{and}$$

$$\hat{\sigma}_{s,2} = \frac{\hat{\sigma}_{s,1}^2\Delta\gamma^2}{8\Gamma_2(\hat{\sigma}_{s,1} - 3\Gamma_3/(2\Gamma_2))}.$$

Since $\Gamma_2 < 0$, the stability condition is $\Gamma_3 > 0$, which holds only for the triad (uss). Combining the analysis of the fast and slow frequencies, the stability condition for a fixed point of the triad under the ordering assumption of Eq. (19) is

$$\Delta\gamma < \frac{3}{2}\frac{\Gamma_3}{\Gamma_2}, \Gamma_2 < 0, \quad \text{and} \quad \Gamma_3 > 0. \quad (20)$$

The stability diagram is shown in Fig. 1. Generally there is a necessary range $\Delta\gamma_{\text{lower}} < \Delta\gamma < \Delta\gamma_{\text{upper}}$ for a stable fixed point.

Before further analysis, it is worth noting that there is a nonlinear limit where the linear frequencies and growth rates are negligible. This limit occurs when the amplitudes are sufficiently large, and leads to a well-known integrable system. This integrable dynamics is observed on a fast time scale, however, with certain modifications on the slow linear time scale. The details are shown in the Appendix for later reference.

IV. SATURATION AND RELAXATION OF A TRIAD

In Sec. III, the stability of a fixed point is investigated in the phase space (Ψ, $\Delta\psi$). The evolution of a triad is now studied with the initial condition $\phi_i = 0.001$. The parameters of the triads investigated are

$$\text{Triad(I)} : \omega_1 = -1.2 + 0.3i, \quad \omega_2 = 0.0 - 0.01i, \quad \omega_3 = -1.3 - 0.4i$$
$$\text{Triad(II)} : \omega_1 = -1.2 + 0.3i, \quad \omega_2 = 0.0 - 0.1i, \quad \omega_3 = -1.3 - 0.25i$$
$$\text{Triad(III)} : \omega_1 = -1.2 + 0.3i, \quad \omega_2 = 0.0 - 0.1i, \quad \omega_3 = -1.3 - 0.2i.$$

The wave vectors are given by

$$k_1 = (0.0, 0.4), \quad k_2 = (0.2, 0.0), \quad k_3 = (-0.2, -0.4),$$

which yields $(M_1, M_2, M_3) = (-0.0128, 0.0032, 0.0097)$. Triad (I) represents the interaction of an unstable drift wave, a marginally stable zonal mode $k_y = 0$ with zero linear frequency, and a stable mode. For comparison, Triads (II) and (III) have slightly different linear growth rates for the second and third modes. The fixed points of Triads (I) and (III) are stable. The fixed point of Triad (II) is unstable.

The amplitudes and the triad phase are shown in time in Fig. 2. Initially each mode evolves linearly, with the triad phase given by $\Delta\psi = t\Delta\omega$. When mode 1 is sufficiently large that $\gamma_3\Phi_3 \simeq M_3\Phi_1\Phi_2$, mode 3 evolves nonlinearly, while modes 1 and 2 evolve linearly. Mode 3 has a phase velocity $-(\omega_1 + \omega_2)$ and a linear growth rate $\gamma_1 + \gamma_2$. The triad phase locks at the value $\Delta\psi = \Delta\psi_1$, where

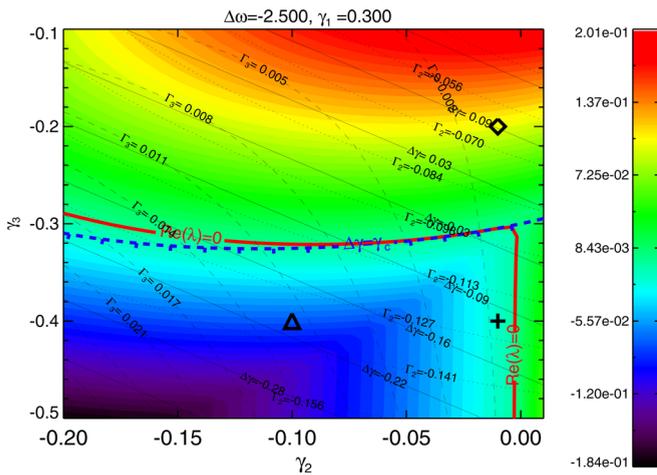$$\Delta\psi_1 = \tan^{-1}\frac{\Delta\omega}{(\gamma_1 + \gamma_2 - \gamma_3)}. \tag{21}$$

This state lasts until $\Phi_2 \sim \Phi_3$. Then the modes 2 and 3 are growing at a rate $\sim \sqrt{\Phi_1^2|M_2M_3|\cos^2\Delta\psi}$. This explosive growth lasts until $\gamma_1\Phi_1 \simeq M_1\Phi_2\Phi_3\cos\Delta\psi \simeq M_1\Phi_2^2\cos\Delta\psi$. At that point, the nonlinear interaction becomes important for mode 1. The large nonlinear terms cause a transition from the linear phase to the nonlinear phase for mode 1, with the transition occurring at $\gamma_1\Phi_1 \sim \alpha\Phi_2\Phi_3 \sim \beta\Phi_1^2$. This transition does not include a secondary instability arising in electron temperature gradient mode (ETG) and ITG turbulence, since the coefficient β is dependent on the linear characteristics of modes 2 and 3. In secondary instabilities, the balance $\gamma_1\Phi_1 \sim \beta_{\text{2nd}}\Phi_1^2$ is dependent only on the linear characteristics of the mode 1, e.g., the eigenmode structure. This transition is relevant to the criteria of Terry et al.[15] However, transition to the nonlinear state and relaxation (or saturation) can show different dynamics, as described in Kim and Terry.[17] In the nonlinear state, each mode relaxes toward the fixed point of the triad because Triad (I) is stable.

What happens if the fixed point of a triad is unstable? The top panel in Fig. 3 shows the evolution of the unstable triad (II). The linear dynamics shows little difference from that of triads (I) and (II). In the nonlinear state, instead of converging toward $\Delta\psi_0$ as in Fig. 2, the triad phase diverges and oscillates rapidly between $\Delta\psi = 0$ and $-\pi$. The amplitudes keep increasing with an exponential growth rate 0.062

FIG. 1. (Color online) Stability diagram of $\Delta\omega = -2.5$ and Im $\omega_1 = 0.3$. The horizontal and vertical axes represent γ_2 and γ_3. The thick blue line (dashed) shows the stability condition $\Delta\gamma = \gamma_c = 3\Gamma_3/2\Gamma_2$ in Eq. (20). The thick red line (solid) shows Re $\sigma = 0$. Triad (I) (+), Triad (II) ($\triangle$), and Triad (III) ($\diamond$) are shown for Sec. IV.
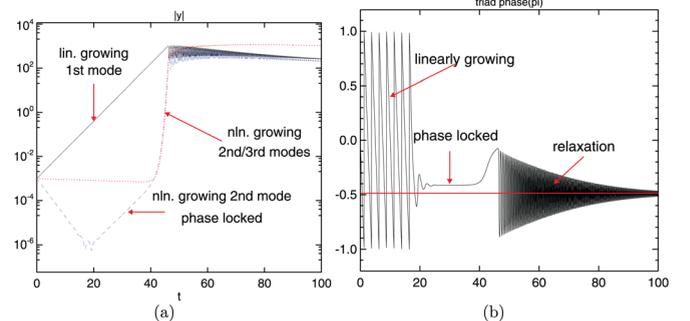

FIG. 2. (Color online) The evolution of the mode energies (left) and the triad phase (right), from the numerical simulations of Eq. (1) for Triad (I). The black (solid), red (dotted), and blue (dashed) traces represent modes 1, 2, and 3. The red horizontal line indicates the triad phase of the fixed point, $\Delta\psi_0$.
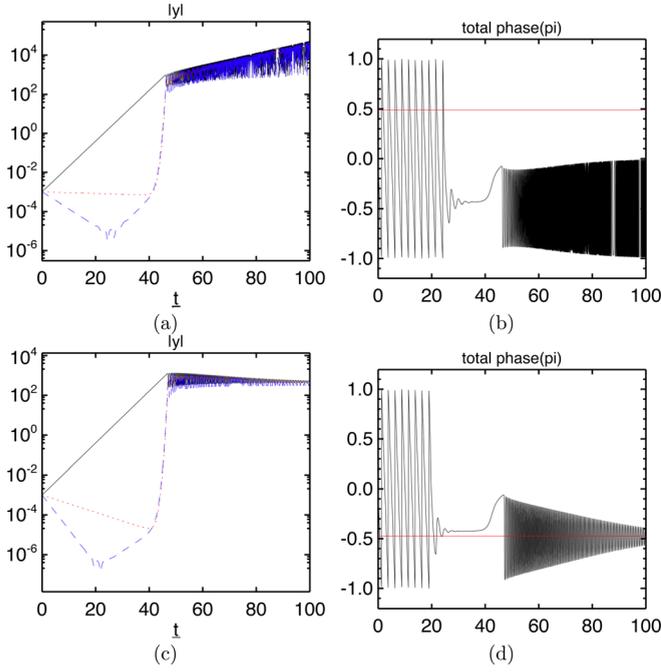
FIG. 3. (Color online) The evolution of the mode energies (left) and the triad phase (right), from the numerical simulations of Eq. (1) for Triad (II) (top) and Triad (III) (bottom). The legends in the plots are described in Fig. 2.

compared to the maximum Re $\sigma = 0.081$. The deviation of the exponential growth rate from the characteristic growth σ of the linear fixed-point stability analysis may be due to the nonlinearity.

As the amplitude of the unstable triad continues to grow (Fig. 4(a)), the rate of change of the triad phase is governed by the nonlinear interaction, proportional to $\sin \Delta\psi$. The dependence leads the triad phase to stay in the neighborhood of $\Delta\psi = 0$ or $\Delta\psi = \pi$, i.e., $\cos \Delta\psi = \pm 1$. On the slow linear time scale, the fast switching of the triad phase between 0 and π seems to act like a random phase and has a stochastic stabilizing effect on the fixed point. When the amplitudes of the mode grow to the point that the nonlinear time scale $N(\varphi)/(d\varphi/dt)$ is much shorter than any linear time scale ω_i, the well-known Jacobian elliptic solutions represent the nonlinear time scale. However, since the fixed point is unstable, the amplitudes keep growing larger continuously and the nonlinear time scale becomes shorter.

In the stable triad, the triad phase converges to the triad phase of the fixed point. Relaxing toward it, the fast oscilla-
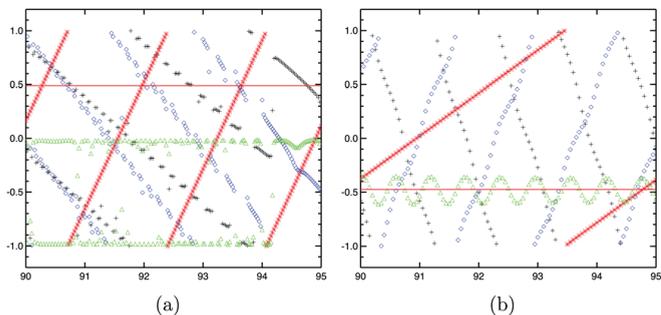

FIG. 4. (Color online) Time evolution of three phases ψ_i [black (+), red (*), blue ($\diamond$)] and the triad phase $\Delta\psi$ [green ($\triangle$)] of the unstable Triad (II) (left) and the stable Triad (III) (right) at $t = 90-95$.

tion in the triad phase $\Delta\psi$ emerges as in Fig. 4(b). This rate is not well matched by either the nonlinear frequency $\hat\omega_i$, or the frequency part Imσ of the linear stability. When the system is further from the fixed point, the triad phase evolves more rapidly. The minimum frequency of the oscillation is the linear frequency of the fixed point, such as $\sigma_f = \sqrt{4\Gamma_2 \tan^2 \Delta\psi}$. It implies that the nonlinear interaction modifies the oscillation significantly during the relaxation. The effect of the nonlinear interaction is hard to quantify. However, it is clear that the shift is larger when the amplitudes of the modes are further away from the fixed point.

From the simulations of Triads (I), (II), and (III), it is clear that the linear analysis of the fixed point is a good indicator whether the fixed point can be reached. An unstable triad tends to grow until the linear properties are negligible, except for its instability, whereas a stable triad has discernible dynamics described by the fixed point and its linear stability.

Even though a fixed point is unstable, it is possible to reason that the properties of the fixed point can be uncovered when the instability of a triad is weak. However, in the long time limit, or when coupled to more triads, it is more likely that the fixed point characteristics are too weak to have a consistent effect on the frequency spectrum. It may contribute to statistically coherent nonlinear energy transfer, i.e., an energy cascade, but whether the fixed point is linearly stable or unstable is a minor issue.

This and Sec. III have explored physical time scales pertaining to triad interaction that are potentially relevant to frequency spectra. We briefly recap the major conclusions before moving on to examine frequency spectra.

(i)   From the fixed point, the frequency of a mode can be shifted from the linear frequency by a nonlinear contribution,

$$\hat\omega_i = \omega_i - \gamma_i \frac{\Delta\omega}{\Delta\gamma}.$$

(ii)   From linear stability analysis of the fixed point, the linear frequencies and growth rates of motion about the triad fixed point is another set of time scales relevant to frequency spectra. These time scales are the slow and fast frequencies of the fourth order characteristic equation,

$$\sigma_f \simeq \sqrt{4|\Gamma_2|^2 \frac{\Delta\omega}{\Delta\gamma}} \quad \text{and}$$
$$\sigma_s \simeq \frac{3\Gamma_3 \pm \sqrt{\Gamma_3(9\Gamma_3 - 4\Delta\gamma\Gamma_2)}}{2\Gamma_2}.$$

(iii)   An integrable solution exists for the limit of large amplitude. Its intrinsic nonlinear time scale derives from the periodicity of the elliptic function and depends on mode amplitudes Ψ_i. It is given by

$$\omega_{\text{amp}} = \frac{2\pi}{T_{\text{amp}}} = \frac{2\pi H \sqrt{m_1}}{2K(m_2/m_1)}, \qquad (22)$$

where, as described in the Appendix, m_1, m_2, and m_3 are linear combinations of $\Psi_i^2/|M_i|$ and $K(k)$ is the

complete elliptic integral of the first kind.[28] The frequency ω_{amp} can be interpreted as a measure of how far the modes are from the trivial fixed point **0**. When the amplitudes are small, $m_1 \to 0$ with fixed m_2/m_1, $\omega_{amp} \sim \sqrt{m_1}$.

V. FREQUENCY SPECTRUM OF A STABLE TRIAD

Before examining the frequency spectra of stable triads, it is useful to introduce one additional time scale that relates to the nonlinear time scale of large amplitude solutions ω_{amp}. Noting that ω_{amp} is a measure of how far the mode amplitudes $\mathbf{\Psi}$ deviate from the trivial fixed point **0**, we adapt the frequency to give a measure of deviation from the nontrivial fixed point $\mathbf{\Psi_0}$. This frequency is

$$\omega_\Delta = \frac{2\pi H \sqrt{\Delta m_1}}{2K(\Delta m_2/\Delta m_1)} \sin \Delta\psi_0, \qquad (23)$$

where Δm_i are identical in form to m_i but with Ψ_i^2 replaced by $(\Psi_i - \Psi_{i0})^2$. The factor $\sin \Delta\psi_0$ is obtained from the expansion of the equations around the fixed point Φ_0. While there is no rigorous justification for this construct, it is found

to have significant concordance with key empirical features of the frequency spectrum. The frequency spectra associated with the time histories of Figs. 3 and 4 are shown in Fig. 5 for various times, in relation to the frequencies discussed above. A frequency spectrum is obtained by taking the complex Fourier transform of the simulation data $\psi_j(t_0 + j\Delta t)(j = 1, n)$ at each t_0. The times $\Delta t = 0.005$ and $n\Delta t = 20.48$ are set to resolve the lowest and highest frequencies among the relevant frequencies. In Fig. 5(e), when the modes have relaxed to the fixed point, the frequency spectrum reasonably replicates the nonlinear frequency $\hat{\omega}_i$.

The frequency spectra can be explained satisfactorily even during relaxation. First of all, the frequency spectra of the modes are well bounded from the upper side by the modulation frequency ω_{amp} even when the transition is highly nonlinear. How far the mode amplitudes are from zero represents the first restriction to the frequency spectrum. However, when only the frequencies from Triad (I) are modified so that $\Delta\omega \sim \Delta\gamma$, the modulation frequency ω_{amp} is a lower bound for the nonlinear frequencies ω_1 and ω_3. Most notably, the spectrum is well bounded by the nonlinear frequency shifted by the relative modulation frequency $\hat{\omega}_i \pm \omega_\Delta$. Far
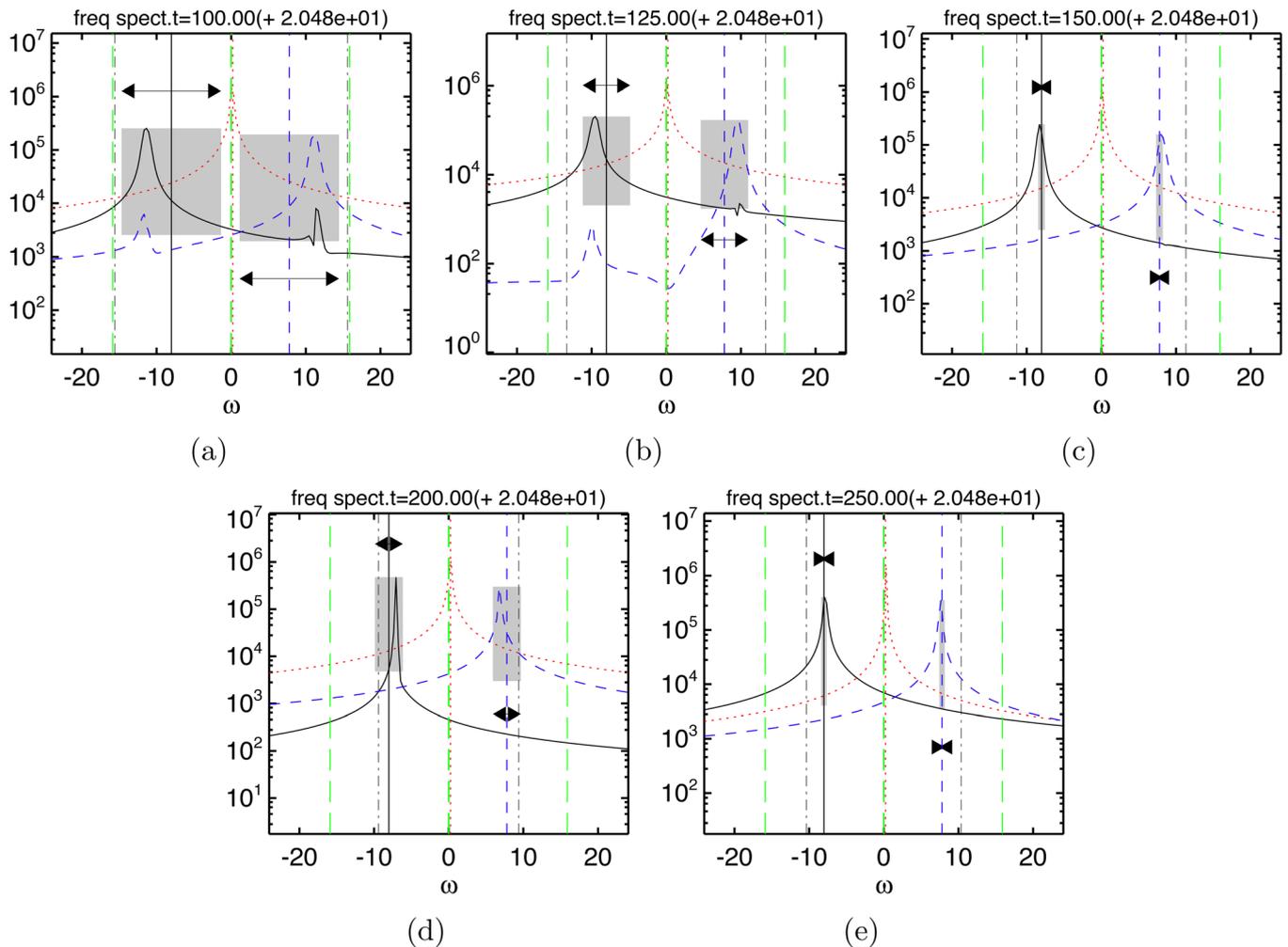

FIG. 5. (Color online) The frequency spectra of the mode ψ_1 (black, solid), the mode ψ_2 (red, dotted) and the mode ψ_3 (blue, dashed) are plotted at $t =$ (a) 100, (b) 125, (c) 150, (d) 200, (e) 250. The vertical lines represent $\hat{\omega}_1$ (black, solid), $\hat{\omega}_2$ (red, dotted), $\hat{\omega}_3$ (blue, dashed), σ_f (green, long dash), and ω_{amp} (black, dash dot). The arrows and the shaded region refer to the interval bounded by $\hat{\omega}_i \pm \omega_\Delta$.

from the fixed point, $\omega_\Delta > |\omega - \hat{\omega}_i|$ may be too broad and loses meaning. When $\omega_\Delta \sim |\hat{\omega}|$, $\hat{\omega}_i \pm \omega_\Delta$ as an estimate of the nonlinear frequency is no longer relevant. However, even though the relevance is questionable when mode amplitudes are too small or large, the specified range describes the spectra over the whole relaxation process.

The spectrum of the second mode φ_2 is sharply peaked and barely changes in time during relaxation. Because $n_i = \Psi^2/|M_i| \sim 1/\gamma_i$, $n_2 \gg n_1, n_3$ holds for the wave action n_i near the fixed point, yielding $m_1 \gg m_2$. The amplitude ϕ_2 is $n_2 \sim (1 + m_2/m_1 \mathrm{sd}^2(\ldots)) \sim 1$ (see Eq. (A4)). n_2 is almost constant. Therefore, the amplitude modulation ϕ_2 is not noticeable in the spectrum.

The triad phase $\Delta\psi$ in Fig. 4 suggests that there should be a signature of the fast eigen-frequency, Im σ_f, in the spectrum. However, it does not appear at any time of the simulations. This is the case because the triad phase is not a phase of any individual mode, and the triad phase oscillation induces the large amplitude changes captured by the frequency estimate ω_Δ.

How robust is the coherent feature of a stable triad? To answer the question, we need to investigate in more detail how the perturbed triad relaxes to the stable fixed point. Figures 6 and 7 show the relaxation in detail. In Fig. 6, the initial triad phase is set to $-\Delta\psi_0$, and the initial mode amplitudes are those of the fixed point, $\Phi_i(0) = \Phi_{0i}$ and $\Delta\psi(0) = -\Delta\psi_0$. The initial values lead to

$$\frac{\mathrm{d}}{\mathrm{d}t}\Psi_i(t=0) = 0 \text{ and } \frac{\mathrm{d}}{\mathrm{d}t}\Delta\psi(t=0) \neq 0.$$

This initial evolution produces a large deviation from the fixed point. However, the system eventually relaxes to the fixed point. It is observed that the triad phase is quickly and
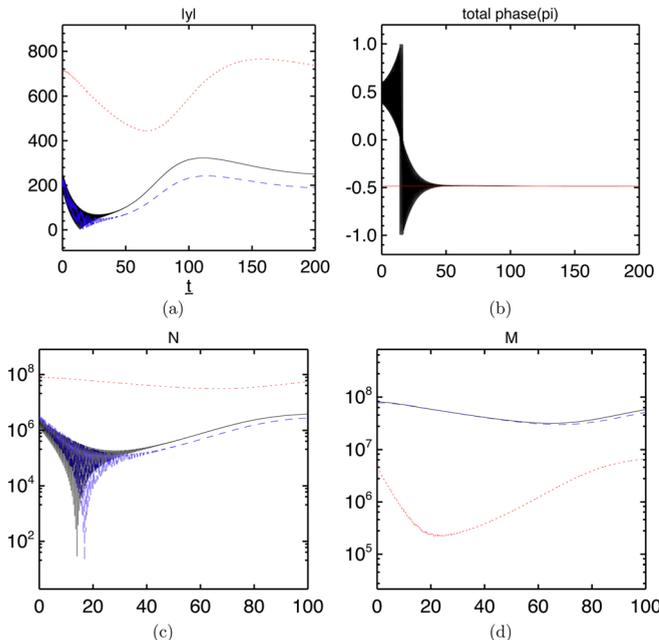

FIG. 7. (Color online) ((a) and (b)) The frequency spectra at $t = 0, 75$ in Fig. 6(c) (Re ϕ_1, Im ϕ_1) at $t = 0, 75$. The legends for the spectra are the same as in Fig. 5 and the red dashed line in (c) and (d) represent the mode 1 at the fixed point.

strongly destabilized; the amplitudes are highly oscillatory until the perturbed triad phase settles to a value near the fixed point, where the sign of sin $\Delta\psi$ is equal to the sign of sin $\Delta\psi_0$. While the amplitudes Ψ_i are highly oscillatory, and therefore, the wave action $n_i \sim \Psi_i^2$, the Manley-Rowe relations Eq. (A2) for m_i is approximately satisfied over the time scale of the fast oscillation. This is the motivation for introducing the frequency of Eq. (23), which bounds the high frequency spectrum near the nonlinear frequency $\hat{\omega}$.

Figure 7 shows spectra and evolution for the initial value $\Phi_i(0) = \Phi_{0u}$ and $\Delta\psi(0) = -\pi - \Delta\psi_0$, which gives

$$\frac{\mathrm{d}}{\mathrm{d}t}\Psi_i(t=0) \neq 0 \quad \text{and} \quad \frac{\mathrm{d}}{\mathrm{d}t}\Delta\psi(t=0) = 0.$$

This figure shows that the initial amplitudes perturbed around the fixed point exhibit nonlinear behavior when they trigger significant change in triad phase. Figures 7(a) and 7(b) demonstrate that the spectra of the nonlinear perturbation follow the prescribed frequency formula. Figure 7(c) shows that the motion is distorted elliptically in the phase space (Re ϕ_1, Im ϕ_1) by an amplitude modulation Φ and the progression of its phase ψ_1. This occurs when the amplitude of the mode 1, Ψ_1, is suppressed from its fixed point value (dashed line).

VI. PERTURBED TRIAD INTERACTION

We have shown, how a stable triad is well described from the properties of its fixed point. In turbulence, any given triad is multiply connected with many other triads. A natural question is whether fixed point properties continue to

FIG. 6. (Color online) The evolution of (a) amplitudes ϕ_i (b) the triad phase $\Delta\psi$ (c) n_i (d) m_i are shown with the initial condition of $\Psi = \Psi_0$ and $\Delta\psi = -\Delta\psi_0$. Black (solid), red (dotted), and blue (dashed) lines in (a,c,d) represent the modes $i = 1, 2, 3$.
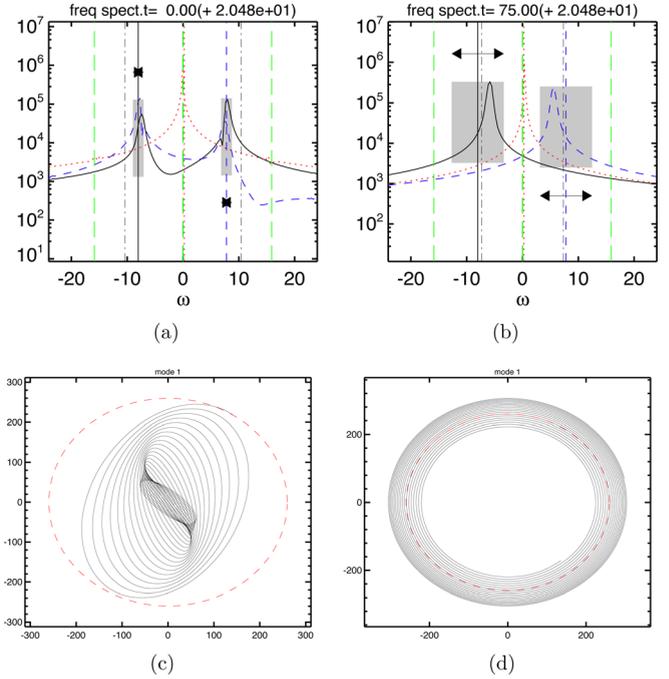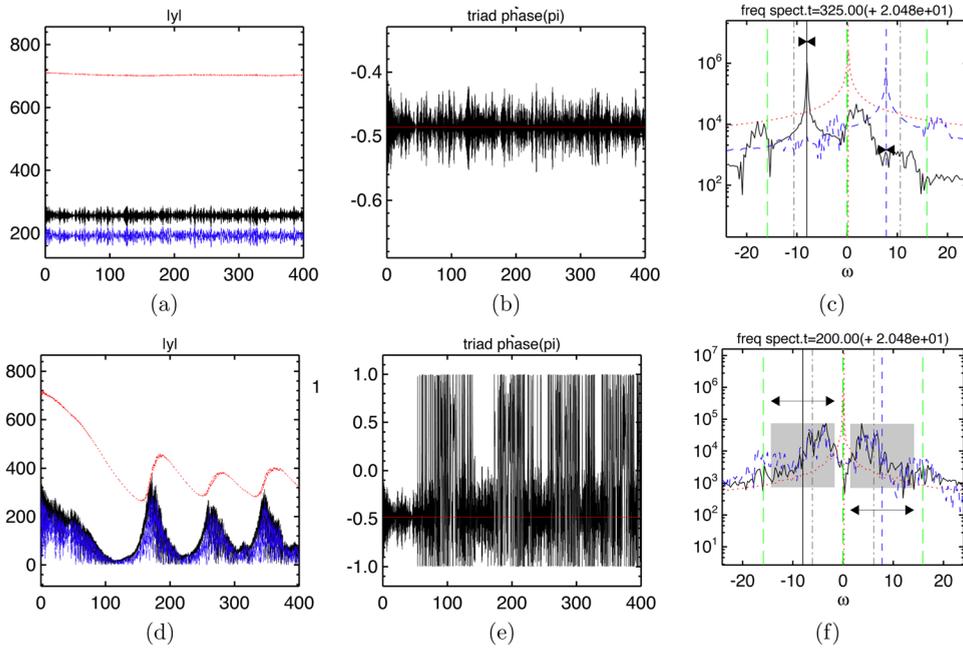
FIG. 8. (Color online) [$\beta = i$] (a and d) Φ_i (b and e) $\Delta\psi$ and (c and f) the frequency spectra at $t = 325$(c) and 200(f). The top panel (a, b, c) and the bottom panel (d, e, f) corresponds to the strength of the perturbation $f_0 = 0.1$ and $f_0 = 0.5$. Each plot has the same legends as described in Figs. 2 and 5.

provide useful information when a triad is connected to other triads.

To provide an answer to this question, a random phase perturbation is applied to only one mode i of the triad in the form

$$\frac{d\phi_i}{dt}(t) + \left[i\lambda_i + \beta \sum_p f_p \sin(\omega_p t + \theta_p)\right]\phi_i = M_i \phi_j^*(t)\phi_k^*(t),$$

(24)

where $f_p = f_0 e^{-[(\omega_p - \omega_{p0})/\Delta\omega_{p0}]^2}$, θ_p is random variable in p, $\beta = 1$ or i, $\omega_{p0} = 10.0$, and $\Delta\omega_{p0} = 2$. The value chosen for ω_p approximately matches the nonlinear time scale in the

triad. The external perturbation leads to either a change in the phase of the mode when $\beta = i$, or the growth rate, when $\beta = 1$.

For $\beta = i$ in a highly nonlinear case with large $\Delta\omega/\Delta\gamma$, the result is independent of the mode to which the perturbation is applied, since the deviation quickly propagates to each mode through the modification of the triad phase $\Delta\psi$. The perturbation is applied to the most linearly stable mode ϕ_3. Figure 8 presents the two cases, with $f_0 = 0.1$ (top) and $f_0 = 0.5$ (bottom). The stability of the fixed point is robust to the external perturbation for small $f_0 = 0.1$. The spectrum is well peaked at its nonlinear frequency $\hat{\omega}$. The amplitudes and the triad phase are fluctuating around the amplitudes of the fixed point. The frequency of the triad phase oscillation
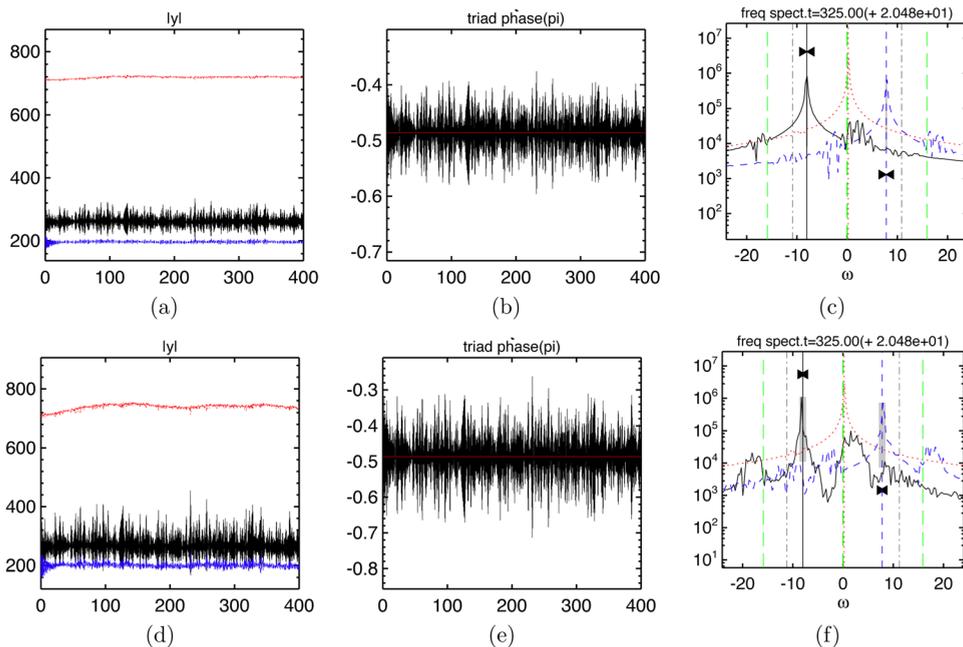

FIG. 9. (Color online) [$\beta = 1$] (a and d) Φ_i (b and e) $\Delta\psi$ and (c and f) the frequency spectra at $t = 325$. The top panel (a, b, c) and the bottom panel (d, e, f) corresponds to the strength of the perturbation $f_0 = 0.1$ and $f_0 = 0.2$. Each plot has the same legends as described in Figs. 2 and 5.
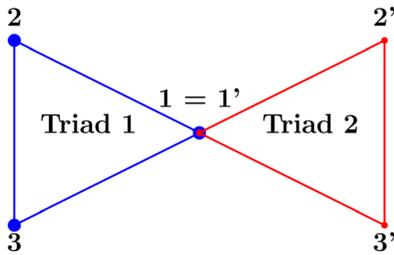
FIG. 10. (Color online) Diagram of two triad connection.

is peaked around the driven frequency ω_{p0}. Varying the driving frequency ω_{p0} from 5, 10, and 20 does not change the response of the triad qualitatively.

Increasing the strength of external perturbation moves the triad away from the fixed point. For $f_0 = 0.5$, the amplitudes are far smaller than the fixed point amplitudes. The triad phase flips sign intermittently. Due to the low amplitudes, ω_Δ is large and has limited utility. However, the small upper bound ω_{amp} restricts the frequency spectrum between $|\omega_{amp}| > |\omega| > |\hat{\omega}| - |\omega_\Delta|$ for $i = 1, 3$.

For $\beta = 1$, the result is dependent on which mode is perturbed. Figure 9 presents results for $f_0 = 0.1$ and 0.2, where the perturbation is applied to ϕ_3. Increasing f_0 leads to large fluctuations around the fixed point. Increasing f_0 beyond the linear growth rate of the perturbed mode $|f_0| > |\gamma_3|$ results in growing mode amplitudes like those of an unstable triad. As long as the strength of the external perturbation does not exceed the linear growth rate, the frequency spectrum is well described by fixed point fixed point properties.

A second approach to the question of triad coupling effects is to connect the two stable triads as in Fig. 10. To ensure that the nonlinearity is conservative, there are two nonlinear terms in each triad at the connecting mode.

Starting with small amplitude initial conditions, one triad tends to dominate the nonlinear energy state unless the complex linear frequencies and nonlinear coefficients of two triads are comparable. In fact, which triad dominates depends on the order of the phase locking in the linear regime.

Starting at the fixed point as the initial condition, the dynamics between two triads are complex and it is difficult to make a simple statement. For simplicity, almost identical triads are investigated. The one triad (1, 2, 3) is Triad (I) and for the other triad (1, 2', 3'), the nonlinear coefficients M'_i for

the triads are the same as M_i of Triad (I), and the linear growth rates γ'_i and wave frequencies ω'_i of the non-connecting linear modes (2', 3') are slightly modified from Triad (I) in such a way of keeping the nonlinear strength, $\tan \Delta\psi$, fixed while varying the stability of a fixed point, Re σ, or vice versa.

As evident in Fig. 11, one triad dominates the other in a short time span $t = O(10)$. The frequency spectrum is well described by the frequency spectrum of the dominant triad. Which triad is dominant is difficult to predict when the two triads have the distinct sets of the complex linear frequencies and nonlinear coefficients. However, if they are nearly identical, it is observed that the triad with the more stable fixed point and weaker nonlinear strength $\tan \Delta\psi = -\Delta\omega/\Delta\gamma$ tends to be dominant. The frequency spectrum is identified with the spectrum of the dominant triad. The interaction of two triads hints that the nonlinear frequency and the amplitudes of a stable triad may be present even in a complex network of triads. More analysis on the interaction among triads needed, but is beyond the scope of the present work.

VII. CONCLUSION

The three-wave coupling model of the complex linear frequencies is investigated for the nonlinear interaction in a triad with linearly unstable and stable modes. Time scales associated with linear and nonlinear physics are identified and compared with features of the frequency spectrum.

The model can reach its own saturation when there is a nontrivial stable fixed point. At saturation, the nonlinear frequency $\hat{\omega}$ is determined by the linear frequency and the nonlinear frequency shift. The nonlinear frequencies $\hat{\omega}_i$ satisfy the frequency matching $\Delta\hat{\omega}_i = 0$, which may be identified as a signature of coherent nonlinear interaction between linearly unstable and stable modes. The mode amplitudes are proportional to the nonlinearity $|\Delta\omega/\Delta\gamma|$ of a triad. While a linearly resonant triad is unlikely to be dynamically coherent because its fixed point is unstable, the modes in the triad may be statistically correlated in multiple connected triads or turbulence. A linearly non-resonant triad can be dynamically coherent in strong turbulence because of the stability of its fixed point. At saturation and in the transient relaxation to the steady state, the spectrum of a mode is well described by the frequencies of the fixed point $\hat{\omega}$ and the amplitude modulation where the action is altered from its usual definition to yield a modified parametric frequency ω_Δ based on the distance from the fixed point. Applying an external perturbation and connecting two triads, we have confirmed that our formula for the frequency range works well in the model. Here we show relevant time scales and dynamical features and conditions in a triad of linearly unstable and stable modes in a simple model of three wave interaction. More practical results require the comparison of a model of at least six modes with the full simulation of relevant turbulence model. This task is left to future work.

These results suggest that the linear frequencies and the linear growth rates of damped modes do create features in the frequency spectrum, i.e., a finite amplitude frequency $\hat{\omega}$, albeit with a nonlinear shift. Clustering of shifted frequencies sets an
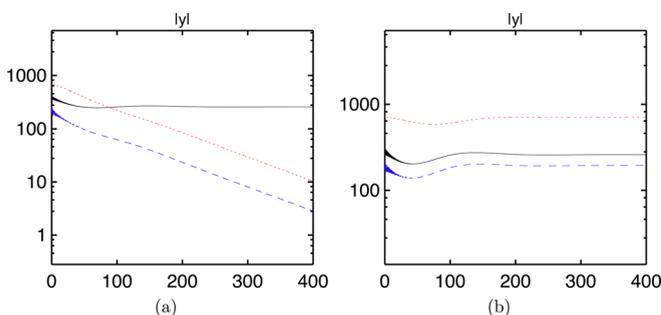

FIG. 11. (Color online) In the case of $\tan \Delta\psi_1 = \tan \Delta\psi_2$ and $\sigma_1 < \sigma_2$, the amplitudes of (a) the modes 1 (black, solid), 2 (red, dotted), 3 (blue, dashed) of triad 1 and (b) the modes 1' (black, solid), 2' (red, dotted), 3' (blue, dashed) of triad 2 are shown in time.

overall spectral envelope that is smoothed and extended by the nonlinearity. There are multiple nonlinear time scales in the triad interaction. Only the empirical modified parametric frequency ω_Δ, in addition to the nonlinear frequency of a fixed point $\hat{\omega}$, has a clear signature in the spectrum. The characteristic frequencies of small amplitude perturbative motion about the fixed point do not correlate with gross spectral features.

These results potentially inform the interpretation of measured fixed-wavenumber frequency spectra. The key caveat is the unknown effect on a single triad from its couplings to all the other triads in the turbulence. Two limited efforts to model the effect of other triads suggest robustness in the single triad results. These were the introduction of random perturbations to the linear growth rate and frequency, and coupling to a second triad. In the latter, the mode with the most stable fixed point tended to make the largest contribution to the spectrum, via the nonlinearly shifted frequency and broadening by ω_Δ. In turbulence, this tendency, if persistent, will be folded together with relative amplitude distributions set by the turbulent energetics. Thus it is premature to draw firm conclusions. One informative test, to be conducted with simulations of a full turbulence model and strong turbulence analytic theory will be to compare this frequency with nonlinear correlation rates from simulation and closures like eddy damped quasinormal Markovian.

ACKNOWLEDGMENTS

APPENDIX: AMPLITUDE MODULATION

When the fixed point of a triad is unstable, the nonlinear term becomes dominant in the evolution of the mode amplitudes. Also it is observed that the triad phase remains at $\Delta\psi = 0, \pi$ so that $\cos \Delta\psi = \pm 1$. Then in case of $\Delta\psi = 0$, Eq. (7) can be approximated by

$$\frac{d\Psi_i}{dt} = M_i \Psi_j \Psi_k.$$

Changing the variable from Ψ_i to $n_i = \Psi_i^2/|M_i|$ gives

$$\frac{dn_i}{dt} = 2 sgn(M_i) H \sqrt{n_i n_j n_k}, \tag{A1}$$

For the triads (uss) and (uus), there are Manley-Rowe relations,

$$\begin{aligned} n_1 \pm n_2 &= m_1 \\ n_1 + n_3 &= m_2 \\ n_2 \mp n_3 &= m_3, \end{aligned} \tag{A2}$$

where m_1, m_2, and m_3 are constants. The former case represents the disintegration of the unstable wave into two stable waves and vice versa ($m_1 = m_2 + m_3$). The latter represents the disintegration of the stable wave into the two stable waves and vice versa ($m_2 = m_1 + m_3$).

The former case becomes

$$\begin{aligned} \frac{dn_1}{dt} &= -2H(n_1 n_2 n_3)^{1/2} = -2H\sqrt{n_1(m_1 - n_1)(m_2 - n_1)}, \\ \frac{dn_2}{dt} &= 2H(n_1 n_2 n_3)^{1/2} = 2H\sqrt{(m_1 - n_2)n_2(n_2 - m_3)}, \\ \frac{dn_3}{dt} &= 2H(n_1 n_2 n_3)^{1/2} = 2H\sqrt{(m_2 - n_3)(m_3 + n_3)n_3}. \end{aligned} \tag{A3}$$

Assume $m_1 > m_2 > m_3 > 0$,

$$-\sqrt{m_1}H(t-t_0) = F\left(\sqrt{\frac{n_1(t)}{m_2}}|k_1\right) - F\left(\sqrt{\frac{n_1(t_0)}{m_2}}|k_1\right),$$

$$\sqrt{m_3}H(t-t_0) = F\left(\sqrt{\frac{n_2(t)-m_3}{m_1-m_3}}|-k_2\right) - F\left(\sqrt{\frac{n_2(t_0)-m_3}{m_1-m_3}}|-k_2\right),$$

$$\sqrt{m_3}H(t-t_0) = F\left(\sqrt{\frac{n_3(t)}{m_2}}|-k_3\right) - F\left(\sqrt{\frac{n_3(t_0)}{m_2}}|-k_3\right),$$

where $F(x; k)$ is the elliptic integral of the first kind,

$$k_1 = \frac{m_2}{m_1} > 0 \quad \text{and} \quad k_1 < 1,$$

$$k_2 = \frac{m_1}{m_3} - 1 > 0,$$

$$k_3 = \frac{m_2}{m_3} > 1,$$

$$F(x; k) = \int_0^x \frac{dy}{(1-y^2)(1-ky^2)}, \tag{A4}$$

$$n_1 = m_2 sn^2\left(-\sqrt{m_1}H(t-t_0) + \theta_1 \Big| \frac{m_1}{m_2}\right),$$

$$n_2 = m_3\left[1 + \frac{m_2}{m_1}sd^2\left(\sqrt{m_1}H(t-t_0) + \theta_2 \Big| \frac{m_2}{m_1}\right)\right],$$

$$n_3 = \frac{m_2 m_3}{m_1}sd^2\left(\sqrt{m_1}H(t-t_0) + \theta_3 \Big| \frac{m_2}{m_1}\right),$$

where θ_i is the initial argument at $t = t_0$ and sn and sd are the Jacobian elliptic function.[28] It should be noted that the oscillatory behavior of n_2 is negligible as $m_2/m_1 \to 0$.

The periods of n_1, n_2, n_3 are the same as

$$T_{\text{mod}} = T_1 = T_2 = T_3 = \frac{2K(m_2/m_1)}{H\sqrt{m_1}}. \tag{A5}$$

The time scale of the dynamics is shorter as m_1 becomes larger. As the ratio $k = m_2/m_1$ increases, the frequency spectrum changes from peaked to broad.

[1]J. Weiland and H. Wilhelmsson, *Coherent Non-Linear Interaction of Waves in Plasmas* (Pergamon, Oxford, 1977).
[2]R. Z. Sagdeev and A. A. Galeev, *Nonlinear Plasma Theory* (Benjamin, New York, 1969).
[3]V. E. Zakharov, V. S. L'vov, and G. E. Falkovich, *Kolmogorov Spectral of Turbulence I—Wave Turbulence*, Series in Nonlinear Dynamics (Springer-Verlag, Berlin, 1992).
[4]M. Rosenbluth, R. White, and C. Liu, Phys. Rev. Lett. **31**, 1190 (1973).
[5]P. Terry and W. Horton, Phys. Fluids **25**, 491 (1982).
[6]J. C. Bowman, J. A. Krommes, and M. Ottaviani, Phys. Fluids B **5**, 3558 (1993).
[7]F. Waleffe, Phys. Fluids A **4**, 350 (1992).
[8]V. S. L'vov, A. Pomyalov, I. Procaccia, and O. Rudenko, Phys. Rev. E **80**, 066319 (2009).

[9]P. H. Diamond, S.-I. Itoh, and K. Itoh, *Modern Plasma Physics, 1: Physical Kinetics of Turbulent Plasmas* (Cambridge University Press, Cambridge, 2010).

[10]R. H. Kraichnan, Phys. Fluids **6**, 1603 (1963).

[11]J. A. Krommes, Phys. Fluids **25**, 1393 (1982).

[12]S. Y. Vyshkind and M. I. Rabinovich, Sov. Phys. JETP **44**, 292 (1976).

[13]J. D. Meiss, Phys. Rev. A **19**, 1780 (1979).

[14]N. Mattor and P. W. Terry, Phys. Fluids B **4**, 1126 (1992).

[15]P. W. Terry, D. A. Baver, and S. Gupta, Phys. Plasmas **13**, 022307 (2006).

[16]D. R. Hatch, P. W. Terry, W. M. Nevins, and W. Dorland, Phys. Plasmas **16**, 022311 (2009).

[17]J.-H. Kim and P. W. Terry, Phys. Plasmas **17**, 112306 (2010).

[18]D. R. Hatch, P. W. Terry, F. Jenko, F. Merz, and W. M. Nevins, Phys. Rev. Lett. **106**, 115003 (2011).

[19]K. Makwana, P. W. Terry, J.-H. Kim, and D. R. Hatch, Phys. Plasmas **18**, 012302 (2011).

[20]D. R. Hatch, P. W. Terry, F. Jenko, F. Merz, M. J. Pueschel, W. M. Nevins, and E. Wang, Phys. Plasmas **18**, 055706 (2011).

[21]J. Candy and R. E. Waltz, Phys. Rev. Lett. **91**, 045001 (2003).

[22]R. E. Waltz, G. M. Staebler, W. Dorland, G. W. Hammett, M. Kotschenreuther, and J. A. Konings, Phys. Plasmas **4**, 2482 (1997).

[23]F. Jenko, W. Dorland, M. Kotschenreuther, and B. N. Rogers, Phys. Plasmas **7**, 1904 (2000).

[24]A. Hasegawa and K. Mima, Phys. Rev. Lett. **39**, 205 (1977).

[25]F. Hinton and W. Horton, Phys. Fluids **14**, 116 (1971).

[26]G. J. Morales and T. M. O'Neil, Phys. Rev. Lett. **28**, 417 (1972).

[27]B. J. Winjum, J. Fahlen, and W. B. Mori, Phys. Plasmas **14**, 102104 (2007).

[28]M. Abramowitz and I. A. Stegun, *Handbook of Mathematical Functions with Formulaes, Graphs, and Mathematical Tables* (Dover, New York, 1972).